Dynamic material properties and terminal ballistic behaviour of shock-loaded silicon-nitride ceramics

H. Nahme, V. Hohler, A. Stilp

Dynamic material properties and terminal ballistic behaviour of shock-loaded silicon-nitride ceramics

H. Nahme, V. Hohler and A. Stilp

Ernst-Mach-Institut, Eckerstrasse 4, 79104 Freiburg, Germany

Résumé

Les effets dynamiques et la structure microscopique des matériaux céramiques de silice-nitride chargées par ondes de choc possédant deux densités différentes ont été examinés à l'aide de l'impact de plaque planar et de la technique VISAR. De plus, le comportement balistique terminal des deux céramiques a été déterminé. Les résultats combinés obténus par les expériences effectuées suggèrent une influence importante de la microstructure sur le comportement balistique terminal et par conséquent sur la capacité de protection des céramiques soumis à l'impact.

Abstract

The dynamic properties and microscopic material structure of shock loaded Silicon-Nitride ceramics of two different densities have been investigated by means of the planar plate impact and VISAR technique. In addition the terminal ballistic behaviour of both ceramics has been determined. The combined results of the tests performed suggest an important influence of the microstructure on the terminal ballistic behaviour and thus on the ceramics protection capability against impact processes.

1. Introduction

For many years a large variety of ceramics have been tested with respect to their protection capability against impact processes /1/. Despite extensive studies, a general relation between the terminal ballistic behaviour and the static and dynamic material properties has still not been established. The studies of the dynamic and terminal ballistic behaviour and the microstructure of Si_3N_4 ceramics having two different densities due to different amounts of porosity presented here are a contribution to this still unresolved problem.

2. Experimental Setup

The dynamic material properties have been determined using the planar plate impact technique /2/ in connection with a VISAR (Velocity Interferometer System for Any Reflector) /3/ and sample recovery techniques. The experimental setup is shown schematically in figure 1. The projectile plates were C45 - steel with a thickness of 3-4 mm and a diameter of 58 mm. The ceramic targets have been plates of 50 mm diameter and thicknesses of $5mm < d_T < 25$ mm. All plates have been prepared to be plane and parallel to better than 0.2 mrad. The tilt between projectile and target at the moment of impact was in the range of 1 mrad. The projectiles have been accelerated using a single stage compressed air gun and a powder gun. The bore diameter of the barrel was 70 mm. Impact velocities in the range $200m/s < v < 1180$ m/s yielded maximum stresses applied to the samples in the range of 2 GPa $< \sigma_{max} < 16$ GPa. By means of the VISAR the velocity history of the target rear surface has been recorded with a time resolution of 2ns.
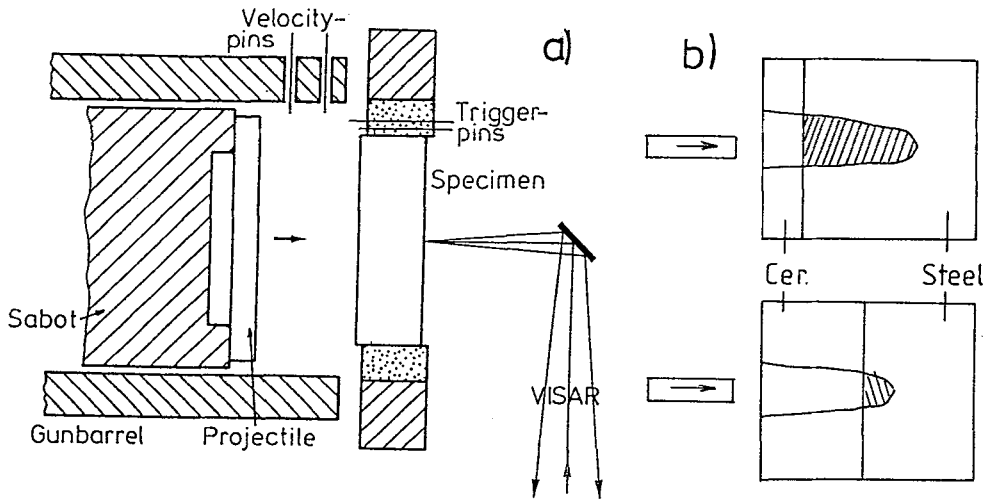
Figure 1: Experimental setup (schematically)
a) plate impact experiments
b) DOP-method

Experiments up to 400m/s impact velocity have been recovery experiments. Sample fragments have been examined by means of scanning electron microscopy.

A brief desciption of wave propagation in shock loaded target plates is given elsewhere in this volume /4/.

The terminal ballistic protection capability of both ceramics have been studied by means of the DOP-method (Depth of Penetration, fig. 1b). With this technique the penetration of a kinetic energy projectile into a steel target is determined for different thicknesses of protecting ceramic layers being located in front of the steel target. A high strength German armor steel of hardness 440 HV_{20} was used. Single ceramic tiles of $130*130$ mm^2 lateral dimension and 18 mm thickness were piled until the required areal density was reached. The gaps between the ceramic tiles have been filled with epoxy, the surfaces were as received from the manufacturer.

The projectiles were made of tungsten-sinter material of density 17.6 g/cm^3, tensile strength of 1.2 GPa and an elongation at fracture of 10%. The projectile diameter was 5.8 mm and the length was 72.5 mm. Impact velocity was around 1700 m/s for all tests.

The densities of the Si_3N_4 samples were 2.28 g/cm^3 and 3.15 g/cm^3 for the porous and the solid material respectively. They will be denoted as 2.28-Si_3N_4 and 3.15-Si_3N_4 in the following text. The longitudinal sound velocities are listed in table 1.

3. Experimental Results and Discussion

Velocity histories measured by the planar plate impact technique are given in figure 2 for both materials. The results for the 3.15-Si_3N_4 are very similar to those known for other ceramics. A high elastic precursor yields a high Hugoniot elastic limit (HEL) and is followed by a further velocity increase due to a "plastic" wave when the stress applied exceeds the HEL significantly. For this material in some cases a clear spall signal has been found. The release wave from the projectile rear surface finally leading to the spall process is in quite good temporal conformity with the values expected from the sample dimensions and known wave velocities.

A completely different behaviour is to be seen for the 2.28-Si_3N_4. All curves exhibit a clear elastic precursor being significantly lower than that of the 3.15-Si_3N_4. A second velocity increase follows with a considerable delay. When the impact velocity is increased to more than 800 m/s and the applied stress exceeds 5.2 GPa, a second sharp structure is observed, followed by a further velocity increase. The spall strength determined from the spall signals sometimes is approximately one half of the strength of the 3.15-Si_3N_4 but in several cases no spall signal was observed. In these cases a small velocity reduction was observed, but the reacceleration process is missing. This indicates, that the shock loaded material is of sufficient internal strength for the release wave to be transmitted, but there is no spall strength left.
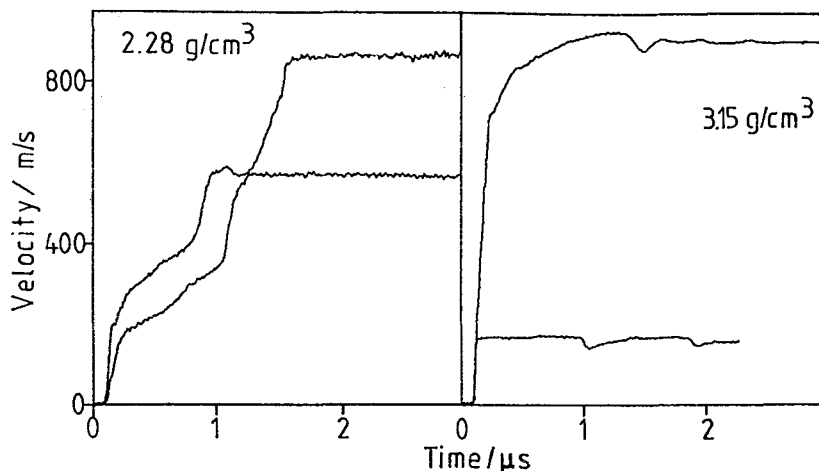
Figure 2: Velocity history curves of Si_3N_4 ceramics

From the amplitude of the elastic precursor u_{HEL} and the velocity decrease due to spallation Δu_{sp} σ_{HEL} and the spall strength σ_{sp} of the materials have been evaluated using

(1) $$\sigma_{HEL} = \rho\, c_l\, u_{HEL}\, /\, 2$$

(2) $$\sigma_{sp} = \rho\, c_l\, \Delta\, u_{sp}\, /\, 2$$

respectively with the initial density ρ and the longitudinal sound velocity c_l. The shock velocity U_s, the maximum stress σ_{max} and maximum strain ϵ_{max} have been calculated using

(3) $$U_s = c_l\, /\, (1 + (c_l\, \Delta t\, /\, d_T))$$

(4) $$\sigma_{max} = \sigma_{HEL} + \rho\, U_s\, (u_{max} - u_{HEL})\, /\, 2$$

(5) $$\epsilon_{max} = ((u_{HEL}\, /\, c_l) + ((u_{max} - u_{HEL})\, /\, U_s))\, /\, 2$$

with the target thickness d_T and the time interval Δt between elastic and plastic wave. The HELs of 2.28-Si_3N_4 depend on the target thickness and exhibit a precursor decay as it is known from some metals /5/.
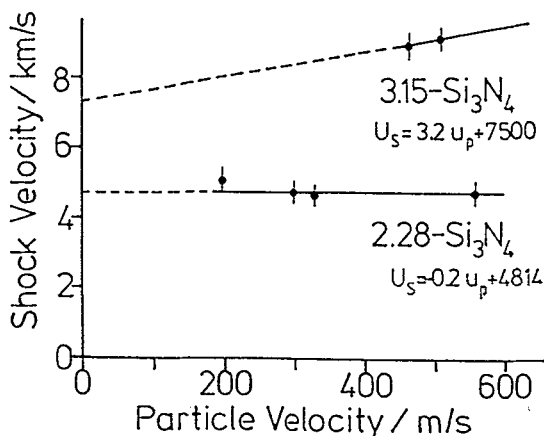

Figure 3: Shock velocity - particle velocity diagram for Si_3N_4 ceramics

In fig. 3 the U_s - u_p data of both materials are displayed. Despite the fact that only for a few tests the HEL was exceeded for 3.15-Si_3N_4 a slightly increasing shock velocity is indicated. The nature of the delay of the second velocity increase for porous 2.28-Si_3N_4 is still questionable. There are four possible explanations for the observed velocity histories:

1. Reflection of the elastic precursor at the plastic wavefront propagating with lower velocity.
2. Reflection of the elastic precursor at a failure wave front.
3. Collapse of the voids and compression of the destroyed material.
4. Behaviour like TiB_2

If reflection of the elastic precursor at the plastic wave front is responsible for the subsequent velocity steps the propagation velocity for the plastic wave front has been calculated from the time intervals between the velocity steps to be 2000m/s< u < 3400m/s. The same calculation holds if the elastic precursor is not reflected at the plastic wave front but at a failure wave propagating into the material. Behind this wave front the material is totally fragmented. This leads to a region of reduced shock impedance reflecting the arriving release wave back to the rear target surface as a pressure wave. This mechanism would be very similar to that observed in glass by and Raiser and Clifton /6/. A collapse of voids normally would lead to a more shallow velocity increase and is in view of the observed sharp structures in the velocity curves improbable. If processes are responsible like in TiB_2 the nature of these processes is still being debated.

From the velocity histories the stress - strain relations given in fig. 4 have been evaluated. Because of the small number of tests only a linear fit has been applied. The fit parameters are also given in table 1.
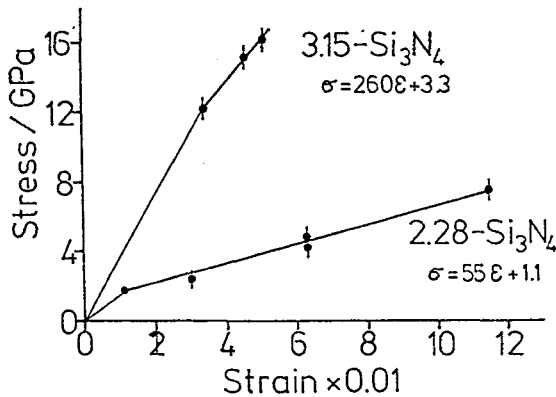

Figure 4: Stress - strain diagram for Si_3N_4 -ceramics

Table 1. Dynamic properties of Si_3N_4 ceramic

ρ=density /g/cm^3, c_l=long. sound speed / m/s, σ_{HEL}=Hugoniot elastic limit / GPa
σ_{sp}=spall strength / GPa, a,b=fitparameter of fig. 3, c,d=fitparameter of fig. 4

ρ	c_l	σ_{HEL}	σ_{sp}	a /m/s	b	c /GPa	d /GPa
3.15	10660	12.1	0.5-0.8	7500	3.2	3.3	260
2.28	8600	1.9	.25	4800	0.2	1.1	55

From the SEM-examination of the microstructure of both materials it can be seen that on a scale of a few microns both materials are of very similar structure. The density difference between both ceramics is due to voids in the range $10\mu m<d<100\mu m$. On a scale below approximately $1\mu m$ the shape of the small particles are somewhat different with edged particles in the case of 3.15-Si_3N_4 (fig. 5a) and smooth particle surfaces in the case of 2.28-Si_3N_4 (fig. 5b). In all sample fragments examined

so far only a few coarse ceramic grains are contained. One of these grains is to be seen in fig.5c. Both types of samples contain regions of glassy resemblance (fig.5d) with an extension of up to several hundred μm. The high number of these regions visible at the fragment surfaces indicate that either there is a high density of these regions spread throughout the material or this glassy material is more susceptible to tension stress than the crystalline ceramic material. Up to 400 m/s impact velocity the material mainly breaks along its grain boundaries. Only few transcrystalline cracks in larger particles have been found (fig.5c).
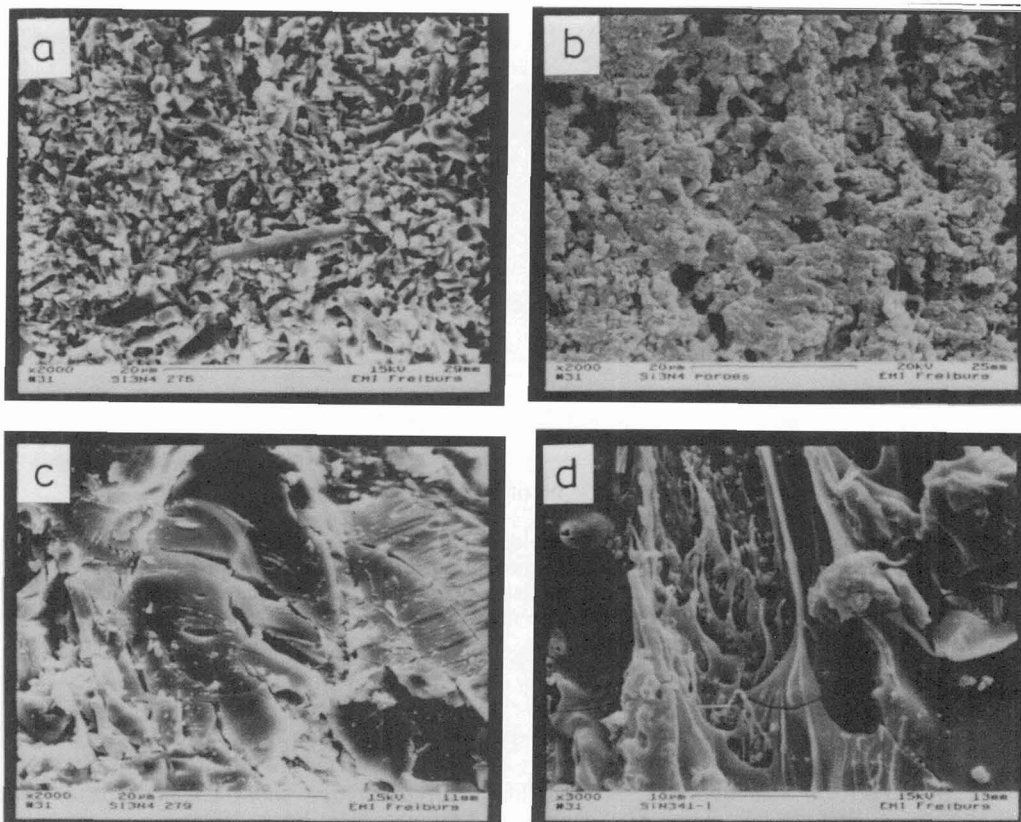

Figure 5: Microstructure of Si_3N_4-ceramics (Description see text)

In fig. 6 the results of the DOP measurements are displayed. For comparison some results of other materials (German armor steel, TiB_2 and Al_2O_3) are included. The penetration depth into the steel target protected by ceramic plates and normalized by the penetration depth without protection is given for varying areal densities of the protecting materials. According to these tests, 3.15-Si_3N_4 belongs to the best protective materials, comparable to SiC and only a little bit less effective than TiB_2. Even the porous 2.28-Si_3N_4 is definitely more effective than Al_2O_3 of the same areal density. Especially at high areal densities the slighty steeper slope of the Si_3N_4 data indicates an improved shielding capability.

One intention of these investigations is a better understanding of the shielding capability of ceramics by combining the results of the terminal ballistic tests and the dynamic material properties. The results for both types of Si_3N_4 show that neither one single dynamic material parameter nor a combination of different parameters can explain the difference in terminal ballistic behaviour of both materials. In addition the difference with respect to other materials can not be explained. However for many of the tested materials the required dynamic values are not known with sufficient accuracy.
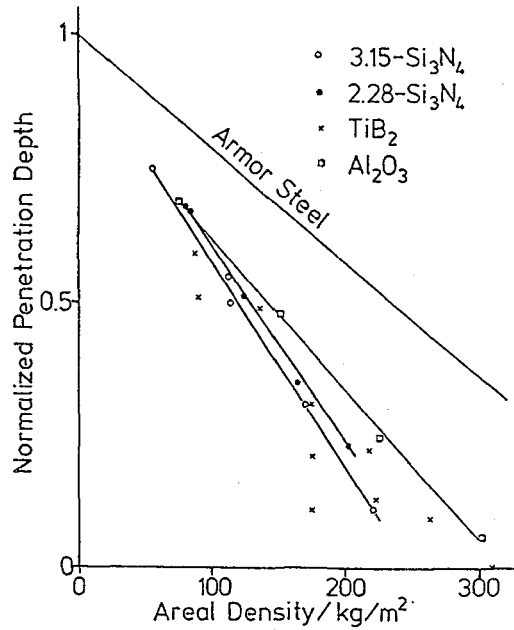
Figure 6: Depth of Penetration results

The SEM-examination of sample fragments yielded that in the microstructure beyond a few microns the structural differences between both materials nearly but not completely vanish. This result and the relatively small differences in the terminal ballistic behaviour despite the large differences in the dynamic properties may be an indication that the material's microstructure plays an important role in the terminal ballistic behaviour of ceramics.

4. References

/1/   M.L.Wilkins, C.F.Cline, C.A.Honodel, "Fourth progress report of light armor program" UCRL-71817 (1969)

/2/   L.M.Barker, M.Shahinpoor, L.C.Chhabildas, *"High-pressure shock compression of solids"* pp.43-73, Editors: J.R. Asay, M. Shahinpoor; Springer, New York, 1993

/3/   L.M.Barker, R.E. Hollenbach, J. Appl. Phys. 43, pp.4669-4675, (1972)

/4/   H. Nahme, M.J. Worswick, this volume

/5/   W. Arnold, Ph.D. Thesis, Technical University Munich, 1991

/6/   G. Raiser, R.J.Clifton, Proc. of the APS-Meeting 1993, Colorado Springs, June 28th- July 2nd. 1993, in press